Flutter Control of Long Span Suspension Bridges in Time Domain Using Optimized TMD

Hamed Alizadeh[1] · Seyed Hossein Hosseni Lavassani[1]

Abstract

Suspension bridges due to their long span are susceptible against dynamic events, like air flow which can cause considerable problems for them. Flutter, as an aerodynamic phenomenon, makes bridges vibrate, whereas their amplitude gradually diverges, needed the vibration control strategies. Tuned mass damper or in brief TMD, as the simplest passive device, can be used for this purpose. The performance of it can be enhanced when it's parameters are adjusted to their optimum values. In this paper, the TMD was optimized by meta-heuristic optimization algorithms to control the flutter of long span suspension bridges. In this regard, the Golden Gate suspension bridge and Car tracking algorithm were selected for case study and optimization process, respectively. Firstly, the flutter analysis of bridge was done by multi-mode method in the time domain, and at second part, the TMD's parameters were simultaneously optimized for maximum increase of flutter velocity of all the vulnerable modes. The results indicated that TMD was perfectly suitable device to control the flutter of long span bridges.

Keywords Suspension bridge · Flutter phenomenon · Time domain · Multi-mode method · Tuned mass damper · Meta-heuristic optimization algorithm

1 Introduction

Suspension bridges are usually the first candidate to connect two far points, creating long spans in their structure. This issue causes that these bridges suffer from the large deformation due to dynamic loads, like wind. They can separately vibrate in four main modes named vertical, longitudinal, lateral, and torsional; also, their vibration can be a combination of mentioned modes (Huang et al. 2005). The prediction of dominant modes of ultimate responses under some events, like ground motions having fortuitous inherent is very difficult. But, this issue about wind is a little different. The deck which air flows around it, can encounter aerodynamic phenomena, like vortex-shedding, galloping, buffeting, static divergence, and flutter (Strommen 2016). Each of the mentioned instances makes bridges vibrate in specific modes, which can be determined in account to occurred phenomenon. For example, flutter makes bridge experience torsional vibration, such that one special mode has the integral role.

Hence, the aerodynamic behavior of suspension bridges should be improved, possible by three main strategies as follows (Li et al. 2015):

(1) Changing the shape of bridge, like using the separate streamlined box girders.
(2) Converting the kinetic abilities by altering the structural configuration of bridge.
(3) Attachment of additional instruments to improve the stability.

Tuned mass damper, as a passive mechanical control strategy, belongs to the third item. In the simplest form, it includes three main parameters called mass ratio, tuning frequency, and damping ratio (Elias and Matsagar 2017). Kwon et al. (2000) utilized a TMD mechanism to activate a plate, changing the air flow around the deck. Their creative passive system was experimentally tested in the wind tunnel test, which was successfully verified. Pourzeynali and Datta (2002) investigated the effects of TMD's parameters on increasing of flutter velocity. The results indicated that TMD did not cause any instability. Finally, the appropriate values of its parameters were informed. Chen and Kareem (2003) investigated the efficiency of TMD for

✉ Seyed Hossein Hosseni Lavassani
lavasani@khu.ac.ir

1 Department of Civil Engineering, Faculty of Engineering, Kharazmi University, Mofatteh Avenue, Tehran, Iran

bridge's flutter control. They tried to introduce a procedure to design optimum TMDs according to the negative damping of structures. Chen and Cai (2004) Suggested a novel control strategy, attenuating the modal coupling effects and mitigating the resonant vibration by TMDs. Abdel-Rohman and John (2006) investigated the performance of TMD in increasing of galloping velocity of flexible suspension bridges without any changes in their shapes. Domaneschi et al. (2015) studied the control of buffeting of suspension bridges using TMD. The results of analysis showed that placing a single TMD at the middle point of the main girder, could reduce the response of bridge. Alizadeh et al. (2018) addressed the sensitivity of flutter velocity into gyration radius and placement of TMDs for the Vincent Thomas suspension bridge. Furthermore, performance of TMD in response reduction of suspension bridges was studied by many researches. (Lavasani et al. 2020a and 2020b; Alizadeh and Lavasani 2020).

Setting of TMD's parameters is the most important factor in designing and controlling process. Efficiency of mass ratio can be improved by increasing the value of it; But, using too heavy TMDs will change the modal properties of structure, while it is not recommended. Damping ratio has less influence compared to mass ratio, however, increasing the value of damping ratio helps to dissipate the more energy of bridge. It is worth noting, that higher values of damping ratio disturb the movement of mass block. Also, mistuning of TMD can considerably decrease its performance (Tao et al. 2017). Hence, the parameters of TMD should be adjusted to their optimum values, needing an optimization process.

Finding the most optimum solution for a certain problem under determined constraints is named optimization process (Chen et al. 2018). Optimization can be done by gradient search methods or meta-heuristic algorithms (Pourzeynali et al. 2007). In the second item, one initial population is created to provide better solution compared to previous one. In other words, it should provide the better generations step by step. Many population-based meta-heuristic optimization algorithms have been introduced and improved by researchers (Rao et al. 2011; Shahruzi et al. 2017). Also, parameters of TMD were optimized in many researches by using these algorithms (Pisal and Jangid 2016; Miguel et al. 2016).

In this paper, flutter analysis of long span suspension bridges is done by the multi-mode method in time domain. TMD, as a passive system, will be optimized in a manner controlling all the existing vulnerable torsional modes. Optimization process will be done according to the highest increase of flutter velocity of related modes. The Golden Gate suspension bridge, as one of the longest ones, located in San Francisco is selected for case study. Also, Car tracking optimization algorithm, as a metaheuristic one, is used as the optimization tool. Finally, the important results obtained by the flutter analysis of bridge, are provided.

2 Flutter Condition

Flutter, as an aerodynamic phenomenon, is divided to two main kinds called two degrees of freedom or classical, and one degree of freedom or torsional, and or A_2^* instability. The first case, common in the airfoil or modern streamlined decks, contains coupling between the vertical and torsional modes. According to the second item's name, A_2^* derivative, related to the torsional degree of freedom, is responsible for flutter. Perhaps, collapse of the first Tacoma Narrows suspension bridge containing wide plate, as the stiffening girder, can be mentioned as the well-known example for this phenomenon (Larsen and Larose 2015). A_2^* can be somehow considered as the sign of stability in the suspension bridges, especially, in truss type ones. When the values of A_2^* are negative, zero or small compared to the structural damping and mass moment of inertia, the occurrence of torsional flutter is impossible. In fact, this type of flutter occurs when the values of A_2^* are positive and have ascendant curvature (Andersen et al. 2016).

During flutter condition in suspension bridges, all modes expose a sinusoidal form of motion. It is worth noting, the number of modes are finite, and generally, one specific mode plays the dominant role. The velocity making zero damping of specific mode, usually the lowest torsional mode, is known as the flutter velocity. At the mentioned velocity, the bridge vibrates due to the self-excited forces, while in lower velocities of flutter, the vibration of bridge will be damped. In higher velocities, one mode will be negatively damped, causing the divergence of vibration's amplitude, which can make the total collapse. The aeroelastic forces, imposed on the deck, are evaluated in account to flutter derivatives named H_i^* and $A_i^*, i = 1 \dots 4$. They were firstly introduced by Scanlan and Tomko (1971) demonstrated in Fig. 1 (Chobsilprakob et al. 2014).

$$L_{se} = \frac{1}{2}\rho U^2 B \left(kH_1^* \frac{\dot{h}}{U} + kH_2^* \frac{B\dot{\theta}}{U} + k^2 H_3^* \theta + k^2 H_4^* \frac{h}{B} \right) \quad (1)$$

$$M_{se} = \frac{1}{2}\rho U^2 B^2 \left(kA_1^* \frac{\dot{h}}{U} + kA_2^* \frac{B\dot{\theta}}{U} + k^2 A_3^* \theta + k^2 A_4^* \frac{h}{B} \right) \quad (2)$$

In which, ρ, U, and B are the air density, wind velocity, and width of deck, respectively. Also, L, M, h, and θ signify lift, torque, vertical, and torsional degrees of freedom, respectively. By the way, sub-index se denotes self-excitation concept.

Fig. 1 a Localized aerodynamic lift force; b localized aerodynamic torque
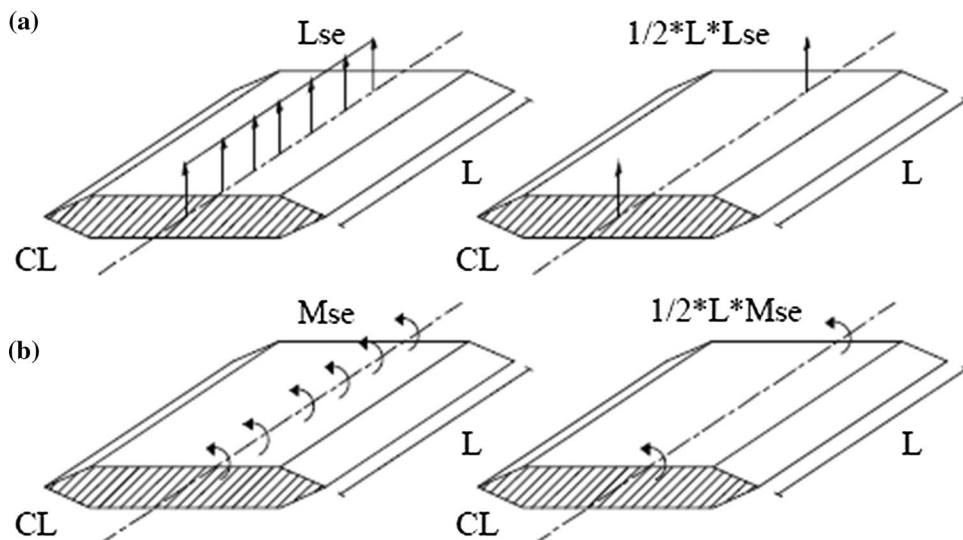
Each flutter derivative affects the certain property of bridge. classical design of suspension bridge includes truss as the stiffening girder. This matter signalizes the role of flutter derivatives related to torsional motion. In this regard, the A_2^* and A_3^* correspond to velocity and rotation of torsion motion, respectively, are the most important ones. As mentioned, A_2^* dissipates mechanical damping, and A_3^* represents the difference between frequencies of flutter and dominant torsional mode.

3 Equation of Motion

Some fundamental assumptions, considered during analysis, are as follows:

(1) Linear behavior is considered during computation.
(2) All the dead load is carried out by the main cables, and the deck does not experience any stress.
(3) The hangers are vertical and inextensible cable, and their loads are uniformly distributed along the deck.

Finite element method is used to evaluate the structural properties matrices. In this regard, the suspended structure is divided to limited certain elements. As regards, inextensible vertical hangers result in same vertical displacement of main cables and girder, considering two nodes at the end parts of center line of girder is enough. Figure 2 demonstrates the arrangement of degrees of freedom. By the way, the effects of shear deformation are neglected.

As seen in Fig. 2, each node of the girder has four degrees of freedom namely vertical displacement, bending rotation, warping, and torsional rotation, shown by h, b, w, and θ, respectively. Hence, the order of structural properties matrices of each element is eight. The lift and torque are imposed
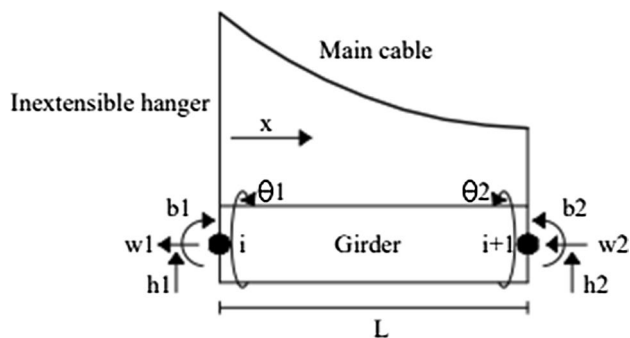
Fig. 2 Finite Element model of suspended structure

at the node i and $i + 1$ in the lumped form. Also, there is not any corresponding force with bending rotation and warping degrees of freedom, meaning zero value. More details about evaluating the structural matrices have been expressed by Rubin et al. (1983) and Lavasani et al. (2020b).

The aerodynamic damping and stiffness can be written according to Eqs. (1) and (2) as follows:

$$C_{ae} = \begin{bmatrix} \alpha_1 H_1^* & \beta_1 H_2^* \\ \beta_1 A_1^* & \gamma_1 A_2^* \end{bmatrix}. K_{ae} = \begin{bmatrix} \alpha_2 H_4^* & \beta_2 H_3^* \\ \beta_2 A_4^* & \gamma_2 A_3^* \end{bmatrix} \qquad (3)$$

where:

$$\alpha_1 = \frac{1}{2}\rho B^2 \omega . \beta_1 = \frac{1}{2}\rho B^3 \omega . \gamma_1 = \frac{1}{2}\rho B^4 \omega \qquad (4)$$

$$\alpha_2 = \frac{1}{2}\rho B^2 \omega^2 . \beta_2 = \frac{1}{2}\rho B^3 \omega^2 H_3^* . \gamma_2 = \frac{1}{2}\rho B^4 \omega^2 \qquad (5)$$

Now, the motion equation can be written by using potential and kinetic energies, and applying Hamilton's principal (Rubin et al. 1983):

$$[M]\{\ddot{x}\} + [C]\{\dot{x}\} + [K]\{x\} = \left[C_{ae}\right]\{\dot{x}\} + \left[K_{ae}\right]\{x\} \quad (6)$$

In which, M, C, and K are the mass, damping and stiffness matrices. Also, x represents the response of degrees of freedom. Equation (6) can be solved by utilizing multimode method in the time domain. Hence, the Cartesian coordinate should be transferred to the modal one:

$$\{x\} = [\Phi]_{m \times m}\{y\}_{m \times 1} \quad (7)$$

where, Φ and y are the mode shape matric and modal amplitude vector, respectively. By replacing the Eq. (7) in Eq. (6), and pre-multiplying in transposed of modal shape matrix:

$$[\tilde{M}]\{\ddot{y}\} + [\tilde{C}]\{\dot{y}\} + [\tilde{K}]\{y\} = [\tilde{C}_{ae}]\{\dot{y}\} + [\tilde{K}_{ae}]\{y\} \quad (8)$$

In which:

$$\tilde{M} = [\Phi]^T[M][\Phi].\tilde{C} = [\Phi]^T[C][\Phi].\tilde{C}_{ae} = [\Phi]^T\left[C_{ae}\right][\Phi] \quad (9)$$

$$\tilde{K} = [\Phi]^T[K][\Phi].\tilde{K}_{ae} = [\Phi]^T\left[K_{ae}\right][\Phi] \quad (10)$$

In the flutter condition, all the participant modes are converted to a sinusoidal response with a unique flutter frequency. So, the following relation is utilized:

$$\{y\} = \left\{\lambda e^{i\omega t}\right\} \quad (11)$$

where, λ is the modal participation factor. Now, the following relation can provide the flutter condition:

$$\left([\tilde{K}] - \omega^2[\tilde{M} + \tilde{K}_{ae}]\right) + i\left([\tilde{C}] - \omega[\tilde{C}_{ae}]\right)\{\lambda\} = 0 \quad (12)$$

Equation (12) represents the well-known eigenvalue problem of a complex matrix. The determinant of it is zero, while the determinant of both real and imaginary parts be simultaneously zero. This condition needs a trial and error process such that by changing the reduced velocity, a unique ω should be appear making zero determinant. Finally, the flutter velocity can be found as follows:

$$U = \frac{B\omega_f}{k_f} \quad (13)$$

In which, sub-index f denotes the flutter condition.

After computing the flutter velocity, the response of bridge can be evaluated in the state space:
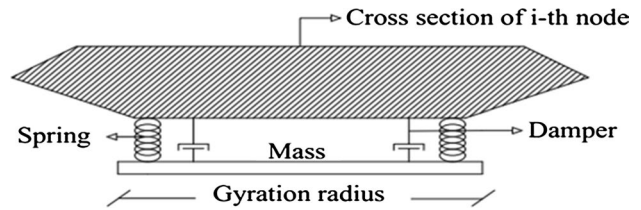
$$\{\dot{z}\}_{2m \times 1} = \begin{bmatrix} 0_{m \times m} & I_{m \times m} \\ \tilde{M}^{-1}\bar{K}_{m \times m} & \tilde{M}^{-1}\bar{C}_{m \times m} \end{bmatrix}\{z\}_{2m \times 1}.\bar{C} = \tilde{C} - \tilde{C}_{ae}.\bar{K} = \tilde{K} - \tilde{K}_{ae} \quad (14)$$

$$\{z\}_{2m \times 1} = \left\{\begin{array}{c} y_{m \times 1} \\ \dot{y}_{m \times 1} \end{array}\right\}.\{x\}_{m \times 1} = [\Phi]_{n \times m} * \{y\}_{m \times 1} \quad (15)$$

I signify unity matrix. Eventually, the ultimate response can be evaluated:

Table 1 Characteristic of used TMD

Parameter	Degree of freedom	
	Vertical	Torsion
Mass	$m_h = m_r m_s$	$I_\theta = m_h r^2$
Damping	$c_h = 2m_h \xi_h \omega_h$	$c_\theta = 2I_\theta \xi_\theta \omega_\theta$
Stiffness	$k_h = m_h \omega_h^2$	$k_\theta = I_\theta \omega_\theta^2$

Fig. 3 Bridge-TMD system

4 TMD Device

Tuned mass dampers were utilized in many studies in order to control the vibrations (Amini and Doroudi 2010; Bortoluzzi et al. 2015; Lievens et al. 2016). Perhaps, the straightforward procedure of designing and low cost of maintaining are the eminent features of it. Vis-a-vis, high sensitivity to mistuning, too much space to place, and immutability of parameters of it versus to dynamic events are the disadvantages of it. However, it is one of the eternal candidate device to control of structures, whether in researches or in practical projects. TMD can be tuned to a specific mode of structure in order to occurrence of resonance to dissipate dynamic energy by its dampers (Debbarma and Das 2016). The most important issue about TMD devices is the setting of its parameters, i.e. mass ratio, damping ratio, and tuning frequency. So, it should be adjusted to its desirable values, which can be achieved by the optimization process. Table 1 and Fig. 3 represent the specifications of TMD utilized in this study.

m_r, m_s, m_h, I_θ denote mass ratio, mass of structure, mass of TMD, and mass polar moment of inertia of TMD, respectively. c, k, and ω sare the damping coefficient of TMD, stiffness of springs, and the frequency of determined mode, respectively, that the sub-indexes specify relevant degree of freedom. The structural properties matrices experience a little change with presence of TMD shown for adding one TMD:

$$[K_{co}] = \begin{bmatrix} AC & AC & AC & \{0\} \\ AC & (K_{AC} + k)_{m \times m} & AC & (-k)_{m \times (n+1)} \\ AC & AB & AC & \{0\} \\ \{0\} & (-k)_{(n+1) \times m} & \{0\} & k_{(n+1) \times (n+1)} \end{bmatrix}_{(n+1) \times (n+1)} \quad (16)$$

$$[C_{co}] = \begin{bmatrix} AC & AC & AC & \{0\} \\ AC & (C_{AC} + c)_{m \times m} & AC & (-c)_{m \times (n+1)} \\ AC & AC & AC & \{0\} \\ \{0\} & (-c)_{(n+1) \times m} & \{0\} & c_{(n+1) \times (n+1)} \end{bmatrix}_{(n+1) \times (n+1)}$$
(17)

$$[M_{co}] = \begin{bmatrix} [M]_{n \times n} & \{0\}_{n \times 1} \\ \{0\}_{1 \times n} & m_{(n+1) \times (n+1)} \end{bmatrix}_{(n+1) \times (n+1)}$$
(18)

AC signifies absolute coefficient of bridge's matrices without attaching TMD. Sub-index *co* denotes combined system of bridge and TMD. Also, *n* represents the number of degrees of freedom.

5 Car Tracking Algorithm

Finding the values of set of parameters to satisfy the needed performance metric under specified constraints is named optimization process. Optimization may be done by the gradient search method, sometimes time consuming; Specially, when the problems are extricated. The other type of methods, inspired from the nature of some physical, biological, and social phenomena are called metaheuristic optimization algorithms which can remarkably decline the time of computation by their random inherent. The last item is renowned to be population-based such that a population of random possible values of parameters, as initial responses, will be improved after determined Repetitions (Mortazavi et al. 2018; Vallada and Ruiz 2011; Chen et al. 2018). Metaheuristic algorithms are widely used to optimize the different range of problems, however, falling in the local extremums is the foible of them. So, designing of these algorithms have been widely developed to overcome the mentioned weakness, which is the important factor in emersion of many new metaheuristic algorithms. In this study, according to the mentioned content, the car tracking algorithm, as a Metaheuristic optimization algorithm, is selected to optimize the parameters of TMD. According to this algorithm, there are N cars in the road on both sides of the origin point looking for the object p. The cars located at the left side of the origin take negative values, while the opposite of mentioned definition is true for the cars located at the right hand. The cars searching for the object p, have two main specifications namely desired velocity (V_n) and their current positions (X_n). All the cars can change their desired velocity to find the object p. When one of the car finds the probably position of the object p, all the cars will move to there to find the exact position of the object p. Considered algorithm optimizes the problems by following steps:

1. Randomly generates the initial car population location shown by X_{ij}. In which, *i* expresses the initial population

and *j* states the number of cars in a population. Here, the optimization process is one-dimensional, *j* is 1.

2. Randomly creates the desired velocity and position of the car population placed at the determined range.

$$X_{ij}(t) = X_{ij} + V_{ij}$$
(19)

3. After initial movement, replaces the car population position into object function to find the probable object p found by the car population.

$$P_i(t) = function(X_i)$$
(20)

4. Finds the best value of objective function, denoting the most probability of finding the object p.

5. In the last step, the car population are divided to two main groups conducting local and global searching to find the best solution.

Car tracking algorithm as a new metaheuristic optimization algorithm is highly competitive compared with the other ones and suitably reduces the time of computation. Fifth step prevents algorithm to fall in local minima, confirming the verification of optimum computed answers. Five steps of mentioned algorithm are briefly defined here, and more details of its computational phases have been represented by Chen et al. (2018).

6 Numerical Analysis

The Golden Gate suspension bridge, placed in San Francisco, is chosen for case study. It is one of the longest bridges in the world with 1281 *m* center span and two 341 *m* symmetric side spans. Stiffening girder is a two hinged truss type which has 7.6 *m* depth and 27 *m* width, and is suspended from the main cables by extensible vertical hangers. The height of both towers is 214.1 *m* and they bear the main cable's load, 17,500 $\frac{kg}{m}$, at the top of themselves. Figure 4 shows the whole structure of it. During computation, side spans are divided to 11 elements, while main span contains 28 elements. Table 2 represents some properties of mentioned bridge and more details are summarized by Rubin et al. (1983).

The modal properties and shapes are provided in Table 3 and Fig. 5.

In order to continue the analysis, the flutter derivatives are drawn according to Scanlan and Tomko (1971) shown in Fig. 6.

It is assumed that the effects of H_4^* and A_4^* are negligible, and also A_1^* is about zero for all reduced velocity $\left(\frac{U}{NB}\right)$. By the way, N is the frequency in account to Hertz. The flutter analysis of bridge is conducted in five independent
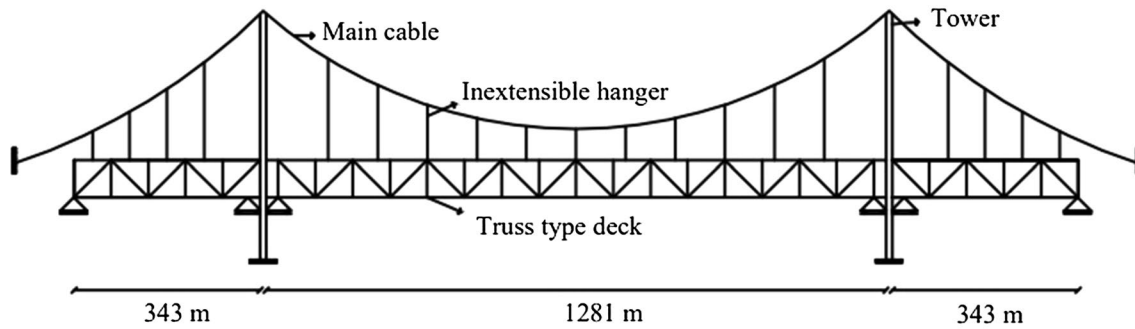
Fig. 4 Total structural view of Golden Gate bridge

Table 2 Properties of Golden Gate suspension bridge

Parameter		Value
Geometric	Length of center span (m)	1280
	Length of Side span (m)	343
	Width of deck (m)	27.45
	Torsion constant of the stiffening structure of side spans (m^4)	1.55
	Torsion constant of the stiffening structure of center span(m^4)	1.55
	Warping constant of the stiffening structure of side spans (m^6)	488.51
	Warping constant of the stiffening structure of center spans (m^6)	757.51
	Virtual length of main cable (m)	2346
	Cross section area of one main cable (cm^2)	5367
Load	Total dead load of side span (kg/m)	17,040
	Total dead load of center span (kg/m)	17,200
	Horizontal tension of the main cable (KN)	237,915
Structural	Modulus of elasticity of the stiffening structure (MN/m^2)	200,027
	Modulus of elasticity of the main cable (MN/m^2)	200,027

Table 3 Modal properties of bridge

Mode no.	Frequency (rad/s)	Period (sec)	Mode type
1	0.59	10.65	V-AS
2	0.77	8.16	V-S
3	0.97	6.48	V-S
4	1.13	5.56	V-AS
5	1.16	5.52	T-AS
6	1.27	4.95	V-S
7	1.32	4.76	T-S
8	1.59	3.95	V-S
9	1.79	3.51	V-S
10	1.82	3.45	T-S
11	2.1	2.99	V-AS
12	2.19	2.87	T-AS
13	2.36	2.66	T-S
14	2.58	2.43	T-S
15	2.6	2.42	V-S

condition, involving different considered number of modes. The results of computation for each condition and participation factors are provided in Tables 4 and 5, respectively.

Table 5 indicates that by increasing considered number of modes, the flutter conveys from lower modes to higher ones and This is due to decrease of the reduced velocity. Hence, opposite of short span suspension bridge, instead of one specific mode, some certain modes should be controlled.

It is recognizable from Table 5, that in each condition, one of the torsional modes plays critical role in the flutter of bridge. First, third and fifth torsional modes are the dominant ones during flutter, respectively. Hence, these modes should be controlled, and a TMD tuned to one of them should guarantee the avoiding of flutter of bridge's vulnerable modes.
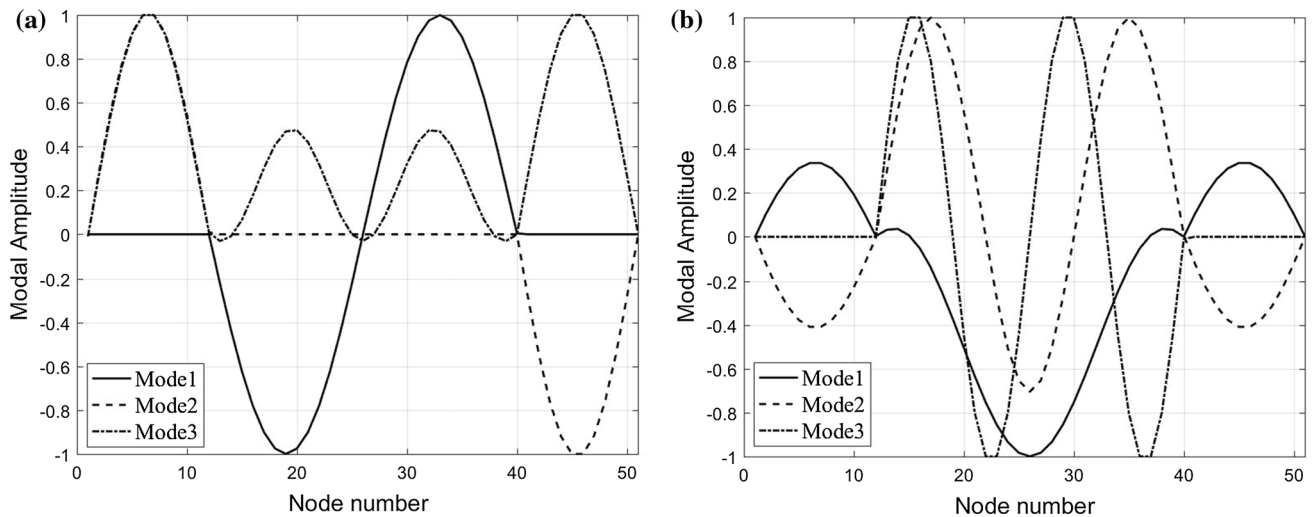
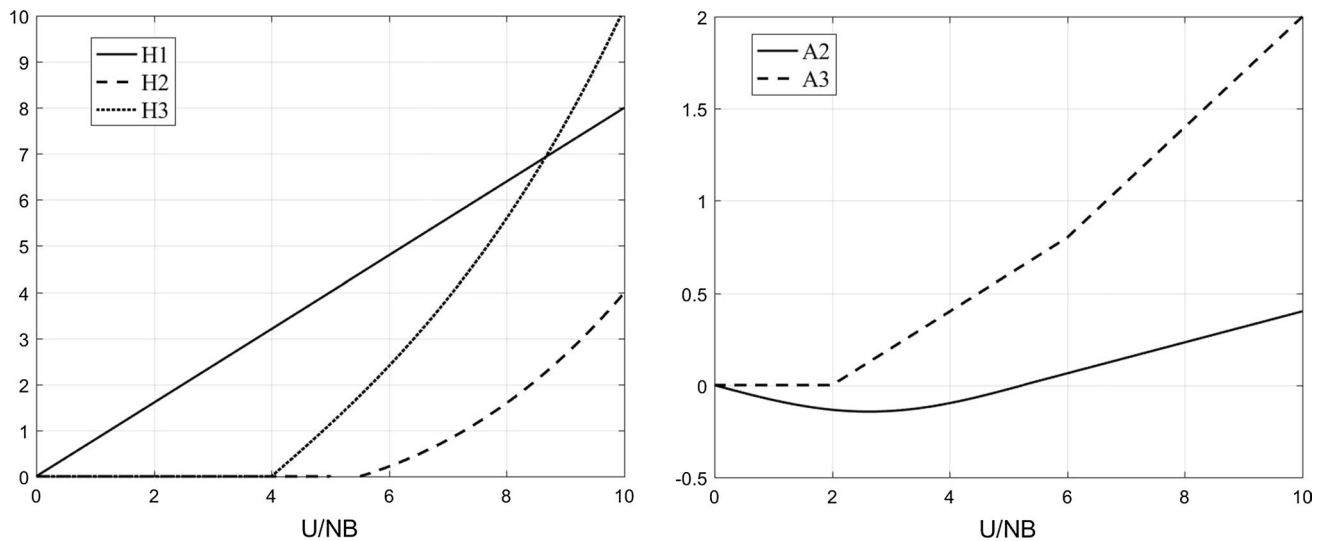**Fig. 5** First three **a** antisymmetric and **b** symmetric mode shapes of bridge

Fig. 6 Flutter derivatives of Golden Gate bridge according to Scanlan and Tomko (1971)

Table 4 Flutter properties of bridge

Condition	Number of modes considered	Flutter frequency (rad/s)	Reduced velocity	Reduced frequency	Flutter speed (m/s)
1	5	1.14	7.95	0.79	39
2	7	1.14	7.95	0.79	39
3	9	1.76	6.21	1.01	47
4	13	2.25	5.8	1.08	56
5	15	2.25	5.8	1.08	56

7 Problem Definition

Flutter condition has been controlled by using many active, semi-active, and hybrid control systems (Xue et al. 2020; Liu 2015; Wen and Sun 2015). These systems can change their characteristics in account to the wind velocity or impose a force, prepared by an external source, in order to control the vibration. For example, when the velocity of wind exceeds from a determined value during using active tuned mass damper (ATMD), an external source will impose forces by its actuators in opposite phase of motion. But, when a passive system is used to control flutter, changing of characteristics or imposing an external

Table 5 Magnitude of modal participation factor

Case / Mode No.	1	2	3	4	5
1	1.7×10^{-4}	1.7×10^{-4}	2.5×10^{-15}	4.1×10^{-6}	4.1×10^{-6}
2	7.6×10^{-15}	5.1×10^{-15}	3.7×10^{-5}	1.3×10^{-15}	1.4×10^{-15}
3	3.5×10^{-15}	3.3×10^{-15}	9.5×10^{-5}	6.3×10^{-16}	8.8×10^{-16}
4	5.9×10^{-16}	2.5×10^{-16}	2.4×10^{-15}	7.9×10^{-16}	8.2×10^{-16}
5	1	1	7.4×10^{-13}	0.1	0.1
6	-	2.2×10^{-5}	1.6×10^{-16}	7.2×10^{-5}	7.2×10^{-5}
7	-	1.7×10^{-11}	0.2	2.3×10^{-12}	4.6×10^{-12}
8	-	-	1.1×10^{-5}	3.5×10^{-16}	4.8×10^{-16}
9	-	-	3.6×10^{-15}	4.6×10^{-16}	3.4×10^{-16}
10	-	-	1	1.5×10^{-12}	1×10^{-4}
11	-	-	-	7.7×10^{-6}	7.7×10^{-6}
12	-	-	-	6.4×10^{-12}	6.4×10^{-12}
13	-	-	-	1	1
14	-	-	-	-	4.6×10^{-12}
15	-	-	-	-	3.6×10^{-16}

force is impossible. TMD, as a passive system, in traditional design, just can control one of the modes of structure which is dominant amongst them. So, how to design of TMDs to control the flutter of long span bridges containing the more torsional spaced modes should be revised. They should be designed in a manner that can control the most vulnerable modes against flutter. On the other hand, TMD does not have the ability to change its parameters under variation of air flow. Hence, here, optimization process should be simultaneously done in a manner that safely avoid flutter concern of specific mentioned modes. In this regard, some considerations are taken account as follows:

(1) Placement of TMDs is specified according to the shape of considered modes. According to this issue, the most important points are $\frac{L_s}{2}$, $\frac{L_c}{6}$, $\frac{L_c}{4}$, and $\frac{L_c}{2}$. Sub-index s and c denote side and center spans, respectively. Also, because of that symmetric geometric of bridge, all the points are specified according to left side and left part of center spans. therefore, the points placed in the right side and right part of center spans will be determined by the symmetry. So, totally seven TMDs may be used to control the flutter. The optimum number of TMDs should avoid flutter concern of mentioned modes.

(2) Parameters of TMDs placed at the different candidate points, have various values which should be optimized.

(3) Instead of tuning of TMDs to a certain mode's frequency, a novel parameter called tuning frequency ratio is introduced. This parameter is ratio of TMD's frequency to the most vulnerable mode's frequency, which is the first mode in this study. it considers the role of all the modes participating in the final response.

(4) It was shown that the effects of vertical modes on the ultimate flutter response is negligible in long span truss type suspension bridges, so the TMDs should be optimized according to its torsional properties. According to Table 1, torsional mass parameter of TMD stated by mass polar moment of inertia contains gyration radius, in addition to mass ratio. So, two independent parameters should be considered.

(5) Considered bridge includes one central and two symmetric side spans that provide various responses. Hence, TMDs should be optimized according to each span's specifications, increasing the parameters that should be optimized.

According to mentioned content, one TMD in each side span and five TMDs in center span may be optimized. TMDs placed at the middle point of side spans have same parameters. This is also true for TMDs placed at $\frac{L_c}{6}$ and $\frac{L_c}{4}$ and their corresponding symmetrical points. As mentioned, totally seven TMDs may be optimized that due to symmetry reduces to four numbers. The considered parameters are separately mass ratio, gyration radius, damping ratio, host nodes, and tuning frequency ratio for each TMD. So, each TMD has five parameters and there are four different TMDs, providing twenty independent parameters which should be optimized. The possible upper and lower bound of parameters are according to Table 6.

Also, the absolute difference of the eigenvalue of real and imaginary parts is selected as the cost-function:

$$f = \left| w_{re} - w_{im} \right| \tag{21}$$

In which, w represents the eigenvalue, and re and im denote real and imaginary parts, respectively. The optimization continues till the value of cost function tends to neighborhood of zero. In this condition, the optimal values of the considered parameters correspond to the maximum value of the reduced velocity. In computation, firstly, value

Table 6 Allowable variation of values of considered parameters

Bound					
Span	Mass ratio (%)	Gyration radius(m)	Tuning frequency ratio	Damping ratio (%)	Host nodes
Side	[0,5]	[0.5,27]	[0.5,1.5]	[1,20]	$\frac{L_s}{4}$
Center	[0,5]	[0.5,27]	[0.5,1.5]	[1,20]	$[0.75\frac{L_c}{6}.1.25\frac{L_c}{6}]$
Center	[0,5]	[0.5,27]	[0.5,1.5]	[1,20]	$[0.75\frac{L_c}{4}.1.25\frac{L_c}{4}]$
Center	[0,5]	[0.5,27]	[0.5,1.5]	[1,20]	$\frac{L_c}{2}$

Table 7 Optimized parameters

Algorithm	Span	Parameter				
		Mass ratio (%)	Gyration radius (m)	Tuning frequency ratio	Damping ratio (%)	Host nodes
Car tracking	Center	2.4	3.3	1.01	10	0.3 L_c, 0.7 L_c
GA	Center	2.5	3.05	1.04	9	0.3 L_c, 0.7 L_c
PSO	Center	2.5	3.1	1.05	8.5	0.3 L_c, 0.7 L_c
TLBO	Center	2.7	3.1	1.1	11	0.3 L_c, 0.7 L_c
OTBLO	Center	2.5	3.2	1.04	9	0.3 L_c, 0.7 L_c

of reduced velocity is fortuitously determined, then the values of specified parameters are randomly assigned. After computation of the first iteration, the set of parameters move toward their optimum values by the mechanism of car-tracking algorithm, which was faster and more accurate compared with other previously used algorithms utilized to optimize the parameters of TMD under seismic excitation (Lavasani et al. 2020a and 2020b; Alizadeh and Lavasani 2020). Also, all the computation has been done in Matlab R2016b.

8 Results and Discussion

Optimization process was simultaneously conducted for all considered variables and modes by various optimization algorithms which are Genetic, Particle swarm, Teaching–learning-based, Observer-teacher-learner-based, and mentioned car tracking (Eberhart and Kannedy 1995; Pourzeynali et al. 2007). The results are provided in Table 7.

All algorithms represent optimum parameters such that can properly increase the flutter velocity. Amongst optimum values, the parameters of mass polar moment of inertia related to the car tracking algorithm is the most optimum. Why so it distributes a lighter mass in a more suitable manner compared to other algorithms. In fact, appropriate distribution of mass block around the torsion axis causes more optimal mass polar moment, however, its mass ratio is the least. This matter is utilized as the selection criterion of optimization algorithm. Table 7 shows that tuning frequency ratio is about 1, indicating the importance of first mode as the most susceptible one. Also, Table 7 does not

Table 8 Flutter properties of combined system

Mode (torsional)	Frequency (rad/s)	Flutter frequency (rad/s)	Reduced velocity	Reduced frequency	Flutter speed (m/s)
1	1.58	1.27	40.17	0.16	223
3	1.57	1.35	26.3	0.24	155
5	2.55	2.1	12.75	0.5	117

inform any TMDs in the side spans, expressing the lower notability of them compared to main span, and in center span just two TMDs is enough, while five TMDs had been predicted. Separating of mass polar moment of inertia to two absolute variables (i.e. gyration radius and mass ratio) makes lighter TMDs, why so optimized gyration radius decreases the mass ratio parameter. By the way, the ratio of optimized gyration radius to width of the deck resulting in 0.12, which can be noted as a practical point during designing of TMD. Host nodes express that two TMDs should be placed at 0.3 L_c and 0.7 L_c points. According to the mentioned results, two optimum TMDs, in account to the mentioned optimum values, are computed for controlling the flutter of considered modes. The novel flutter properties of bridge are summarized in Table 8.

Comparison of differences between frequencies and flutter frequencies in Tables 4 and 8, indicates that A_3^* derivatives affects more considerably combined system. In other words, it has higher rate of depreciation of stiffness. Also, because of that considering first mode as the basis of computation, the corresponding flutter velocity of it noticeably

increases. Needless to say, the other modes experience increasing of flutter velocity too. Optimum parameters of TMDs and the corresponding flutter velocity evaluated here and by other researchers are listed in Table 9.

Based on Table 9, the suggested TMDs of present study provide the highest flutter velocity. The configuration of two first cases is identical; But, tow last cases utilized TMDs in a different manner, perfectly explained by Kwon and Park (2004). Case four suggested five TMDs that the sum of their mass ratio is 3%, providing the lightest TMD. Case 1 reports a slightly larger mass ratio compared to case 4 (its mass ratio was represented according to the whole weight of bridge); Also, case 2 proposed 3 TMDs that their total mass ratio is 9%, providing the heaviest one. About damping ratio, the differences are not remarkable. All cases determine the first torsional mode as the dominant one and specify nearly same frequency ratio. Case 3 and 4 did not ascertain any optimum location to place the TMDs. Case 2 introduced the middle point of spans as the optimal points which may be not correct in long suspension bridges like Golden Gate (represented mode shapes in Fig. 5 verify this issue). In fact, the optimal possible range that host nodes are placed them should be determined based on mode shapes. The highest flutter velocity is achieved by utilizing the corresponding parameters of case 1.

Figure 7 shows the absolute maximum response of bridge's node based on each dominant mode in their corresponding flutter velocity in both controlled and uncontrolled conditions.

Figure 7 indicates that two optimized TMDs could successfully reduce the response of central span in mode one. About third mode the response of side and side part of center spans were considerably reduced, and middle part of center span demonstrates the necessity of an additional TMD. Of course, increasing of bridge's weight should be avoided. On the other hand, the flutter velocity has been adequately increased for this mode. Fifth mode reveals that receding from mode one, designated for tuning frequency of TMDs, reduces the performance of TMD. However, flutter velocity of this mode is placed at the safe point.
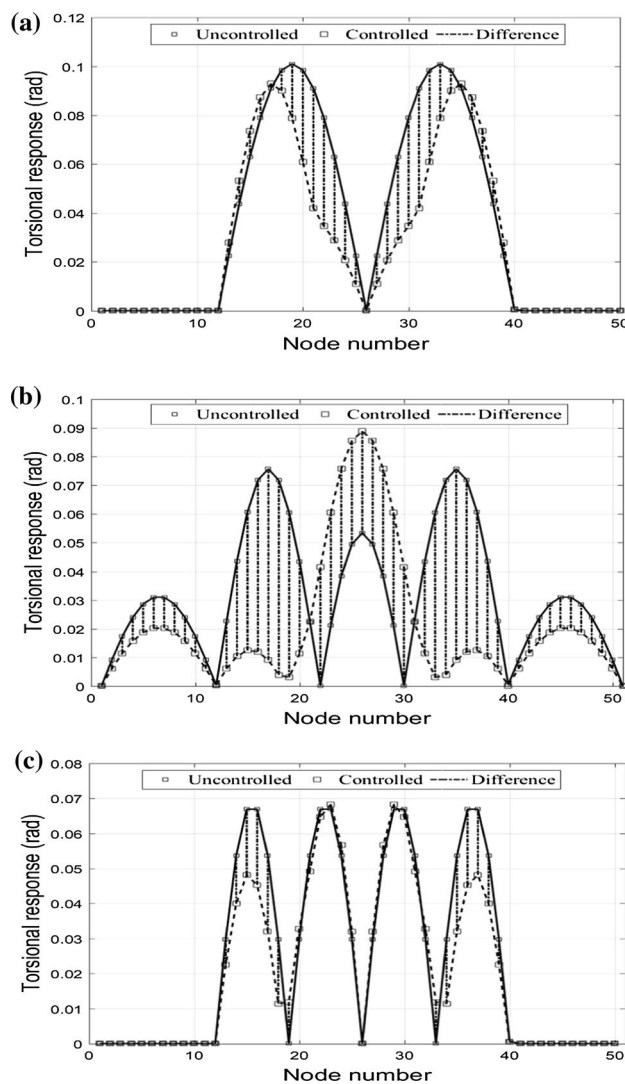

Fig. 7 Total response of bridge along the spans

9 Conclusion

In this study, the flutter analysis of long span suspension bridges was conducted by multi-mode method in time

Table 9 Computed values for TMD system

Case	Research	Bridge	Number of TMD	Mass ratio (%)	Damping ratio (%)	Dominant mode	Frequency ratio (%)	Host nodes	Flutter velocity (m/s)
1	Present study	Golden Gate	2	1.9	10	First torsional	1.01	0.3 L_c, 0.7 L_c	223
2	Pourzeynali and Datta (2002)	Vincent Thomas	3	3	10–20	First torsional	0.8	0.5 L_s 0.5 L_c 0.5 L_s	102
3	Gu et al. (1998)	Sectional model of Tiger Gate	1	5.6	8	First torsional	0.98	–	25.2
4	Kwon and Park (2004)	Golden Gate	5	0.6	–	First torsional	–	–	67

domain. Subsequently, the TMD, optimized by metaheuristic optimization algorithms, was utilized to control the flutter. The Golden Gate suspension bridge and car tracking algorithm were chosen for case study and optimization process, respectively. The most important results can be listed as follows:

In long span suspension bridges, more initial torsional modes are vulnerable against flutter concern. Utilized Control systems should properly prevent the occurrence of flutter condition from the vulnerable modes.

The effect of A_3^* derivatives on dissipating of stiffness matrix of combined system is higher compared to pure bridge.

In long span suspension bridges, maybe some spaced modes play dominant role in various reduced velocity, so all of them should be controlled. In this regard, the TMD's parameters should be optimized according to the first mode's properties, which is reasonable.

Optimization of mass polar moment of inertia in two independent phases related to gyration radius and mass ratio parameters, makes lighter TMD which is desirable. Also ratio of gyration radius to deck's width, 0.12 for the Golden Gate bridge, can be noticed for designing of TMD in long span suspension bridges.

The center span of long span bridges has the dominant role during flutter and the best place of attaching TMD to it is between $\frac{L_c}{4}$ and $\frac{L_c}{2}$ from the each tower; The best point can be find by the optimization process which was 0.3 L_c and 0.7 L_c for the Golden Gate bridge.

Optimized passive TMD controlling three different torsional modes suitably increased the corresponding flutter velocities, and also reduced the maximum response of each node.

References

Abdel-Rohman, M., & John, M. J. (2006). Control of wind-induced nonlinear oscillations in suspension bridges using a semi-active tuned mass damper. *Journal of Vibration and Control, 12*(10), 1049–1080.

Alizadeh, H., & Lavasani, H. H. (2020). TMD parameters optimization in different length suspension bridges using OTLBO algorithm under near and far field ground motions. *Earthquakes and Structures, 30*(5), 625–635.

Alizadeh, H., Lavasani, H. H., & Pourzeynali, S. (2018). Flutter instability control in suspension bridge by TMD. Proceedings of the 11th International Congress on Civil Engineering, Tehran, Iran, May.

Amini, F., & Doroudi, R. (2010). Control of a building complex with magneto-rheological dampers and tuned mass damper. *Structural Engineering and Mechanics, 36*(2), 181–195.

Andersen, M. S., Johansson, J., Brandt, A., & Hansen, S. O. (2016). Aerodynamic stability of long span suspension bridges with low torsional natural frequencies. *Engineering Structures, 120,* 82–91.

Bortoluzzi, D., Casciati, S., Elia, L., & Faravelli, L. (2015). Design of a TMD solution to mitigate wind-induced local vibrations in an existing timber footbridge. *Smart Structures and Systems, 16*(3), 459–478.

Chen, J., Cai, H., & Wang, W. (2018). A new metaheuristic algorithm: car tracking optimization algorithm. *Soft Computing, 22*(12), 3857–3878.

Chen, S. R., & Cai, C. S. (2004). Coupled vibration control with tuned mass damper for long-span bridges. *Journal of Sound and Vibration, 278*(1), 449–459.

Chen, X., & Kareem, A. (2003). Efficacy of tuned mass dampers for bridge flutter control. *Journal of Structural Engineering, 129*(10), 1291–1300.

Chobsilprakob, P., Kim, K. D., Suthasupradit, S., & Manovachirasan, A. (2014). Application of indicial function for the flutter analysis of long span suspension bridge during erection. *International Journal of Steel Structures, 14,* 185–194.

Debbarma, R., & Das, D. (2016). Vibration control of building using multiple tuned mass dampers considering real earthquake time history. *International Journal of Civil and Environmental Engineering, 10*(6), 694–704.

Domaneschi, M., Martinelli, L., & Po, E. (2015). Control of wind buffeting vibrations in a suspension bridge by TMD: Hybridization and robustness issues. *Computers and Structures, 155,* 3–17.

Eberhart, R. C., & Kannedy, J. (1995). A new optimizer using particle swarm theory. In Proceedings of the sixth international symposium on micro machine and human science, Nagoya, Japan, Piscataway: IEEE.

Elias, S., & Matsagar, V. (2017). Research developments in vibration control of structures using passive tuned mass dampers. *Annual Reviews in Control, 44,* 1–28.

Gu, M., Chang, C., Wu, W., & Xiang, H. (1998). Increase of critical flutter wind speed of long-span bridges using tuned mass dampers. *Journal of Wind Engineering and Industrial Aerodynamics, 73,* 111–123.

Huang, M. H., Thabiratnam, D. P., & Perera, N. J. (2005). Vibration characteristic of shallow suspension bridge with pre-tensioned cables. *Engineering Structures, 27*(8), 1220–1233.

Kwon, S. D., Jung, M. S. S., & Chang, S. P. (2000). A new passive aerodynamic control method for bridge flutter. *Journal of Wind Engineering and Industrial Aerodynamics, 86*(2–3), 187–202.

Kwon, S. D., & Park, K. S. (2004). Suppression of bridge flutter using tuned mass dampers based on robust performance design. *Journal of Wind Engineering and Industrial Aerodynamics, 92,* 919–934.

Larsen, A., & Larose, G. L. (2015). Dynamic wind effects on suspension and cable-stayed bridges. *Journal of Sound and Vibration, 334,* 2–28.

Lavassani, H. H., Alizadeh, H., Doroudi, R., & Homami, P. (2020a). Vibration control of suspension bridge due to vertical ground motions. *Advances in Structural Engineering, 23*(12), 2626–2641.

Lavassani, H. H., Alizadeh, H., & Homami, P. (2020b). Optimizing tuned mass damper parameters to mitigate the torsional vibration of a suspension bridge under pulsetype ground motion: A sensitivity analysis. *Journal of Vibration and Control, 26*(11–12), 1054–1067.

Li, K., Ge, Y. J., Gue, Z. W., & Zhao, L. (2015). Theoretical framework of feedback aerodynamic control of flutter oscillation for long-span suspension bridges by the twin-winglet system. *Journal of Wind Engineering and Industrial Aerodynamics, 145,* 166–177.

Lievens, K., Lombaert, G., De-Roeck, G., & Van-den-Broeck, P. (2016). Robust design of a TMD for the vibration serviceability of a footbridge. *Engineering Structures, 123,* 408–418.

Liu, T. (2015). Classical flutter and active control of wind turbine blade based on piezoelectric actuation. *Shock and Vibration, 2015,* 13.

Miguel, L. F. F., Lopez, R. H., Torii, A. J., Miguel, L. F. F., & Beck, A. T. (2016). Robust design optimization of TMDs in vehicle-bridge coupled vibration problems. *Engineering Structures, 126,* 703–711.

Mortazavi, A., Togan, V., & Nuhoglu, A. (2018). Interactive search algorithm: A new hybrid metaheuristic optimization algorithm. *Engineering Applications of Artificial Intelligence, 71,* 275–292.

Pisal, A. Y., & Jangid, R. S. (2016). Vibration control of bridge subjected to multiaxle vehicle using multiple tuned mass friction dampers. *International Journal of Advanced Structural Engineering, 8*(2), 1–15.

Pourzeynali, S., & Datta, T. K. (2002). Control of flutter of suspension bridge deck using TMD. *Wind and Structure, 5*(5), 407–422. https://doi.org/10.12989/was.2002.5.5.407.

Pourzeynali, S., Lavasani, H. H., & Modarayi, A. H. (2007). Active control of high rise building structures using fuzzy logic and genetic algorithms. *Engineering Structures, 29*(3), 346–357.

Rao, R. V., Savsani, V. J., & Vakharia, D. P. (2011). Teaching-learning-based optimization: a novel method for constrained mechanical design optimization problems. *Comput-Aided Design, 43*(3), 303–315.

Rubin, L. I., Abdel-Ghaffar, A. M., & Scanlan, R. H. (1983). Earthquake response of long-span suspension bridge. Research Report No. 83-SM-13; Department of civil engineering, Princeton University, Princeton, United States.

Scanlan, R. H., & Tomko, J. J. (1971). Airfoil and bridge deck flutter derivatives. *Journal of the Engineering Mechanics, 97,* 1717–1737.

Shahrouzi, M., Aghabagloua, M., & Rafiee, F. (2017). Observer-teacher-learner-based optimization: An enhanced metaheuristic for structural sizing design. *Structural Engineering and Mechanics, 62*(5), 537–550.

Strommen, E. N. (2016). *Theory of bridge aerodynamics* (2nd ed.). Netherland: Springer.

Tao, T., Wang, H., Yao, C., & He, X. (2017). Parametric sensitivity analysis on the buffeting control of a long-span triple-tower suspension bridge with MTMD. *Applied Science, 7*(4), 395.

Vallada, E., & Ruiz, R. (2011). Genetic algorithms with path re linking for the minimum tardiness permutation flowshop problem. *Omega, 38,* 57–67.

Wen, Y. K., & Sun, L. M. (2015). Distributed ATMD for Buffeting Control of Cable-Stayed Bridges Under Construction. *International Journal of Structural Stability and Dynamics, 15*(3), 1450054.

Xue, Y., Li, J., Li, F., & Song, Zh. (2020). Flutter and thermal buckling properties and active control of functionally graded piezoelectric material plate in supersonic airflow. *Acta Mechanica Solida Sinica, 33,* 692–706.